

Diode-pumped cw Tm^{3+} : YAlO_3 laser

N.I. Borodin, P.V. Kryukov, A.V. Popov, S.N. Ushakov, A.V. Shestakov

Abstract. The output parameters of a Tm^{3+} : YAlO_3 laser pumped by laser diodes in the spectral region 802–810 nm are studied. The output cw power exceeded 10 W for the total efficiency above 30%. The laser wavelength varies in the range from 1946 to 1985 nm and is determined by the pump power and resonator losses in this spectral region. The efficiency of cross relaxation process during the population of the $^3\text{F}_4$ laser level is measured.

Keywords: yttrium orthoaluminate, cw lasing, diode pumping, laser transition gain.

1. Introduction

Solid-state lasers emitting in the two-micron spectral region have found practical applications in medicine and technology, as well as in laser measuring systems [1, 2]. Diode-pumped Tm^{3+} -doped crystal lasers are of special interest because they feature a high conversion efficiency of pump to laser radiation due to the cross relaxation mechanism of inverse population upon optical excitation of the Tm^{3+} ions into the $^3\text{H}_6 - ^3\text{H}_4$ absorption band. In this case, a pump photon absorbed at the $^3\text{H}_6 - ^3\text{H}_4$ transition of the Tm^{3+} ion interacts with an unexcited Tm^{3+} ion according to the $^3\text{H}_4 - ^3\text{F}_4$, $^3\text{H}_6 - ^3\text{F}_4$ scheme (Fig. 1) by producing the two excited $^3\text{F}_4$ states of the Tm^{3+} ions [3, 4]. Therefore, if a crystal matrix, the activator concentration, and the pump intensity are properly selected, the quantum efficiency of such excitation can be close to 2. In Tm^{3+} :YAG and Tm^{3+} :YLF crystals, which are commonly used in diode-pumped lasers, the most intense absorption lines corresponding to the $^3\text{H}_6 - ^3\text{H}_4$ transition lie in the region 785–795 nm, which allows the use of gallium-aluminium arsenide laser diodes for pumping.

Tm^{3+} -doped yttrium orthoaluminate (Tm^{3+} : YAlO_3) is a promising active material for diode-pumped lasers emitting in the 2- μm region. Because of the crystal anisotropy

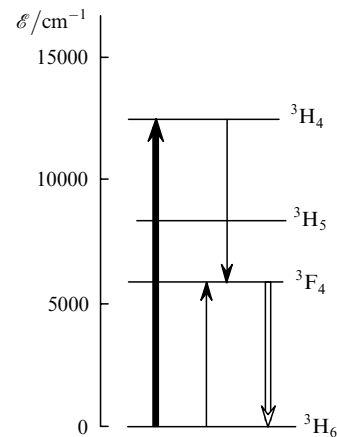


Figure 1. Energy level diagram of the Tm^{3+} ion involved in the production of the inverse population of the upper $^3\text{F}_4$ laser level.

caused by birefringence, the YAlO_3 active elements will experience a small influence of thermally induced birefringence upon pumping. The cross section for the $^3\text{F}_4 - ^3\text{H}_6$ lasing transition is approximately twice that for YAG crystals [5]. The mechanical, thermal, and optical parameters of the YAlO_3 crystals are also favourable for their applications in lasers [6].

The output characteristics of a longitudinally diode-pumped Tm^{3+} : YAlO_3 laser (with the concentration of Tm^{3+} ions $C_{\text{Tm}} = 4.2\%$) operating on the $^3\text{F}_4 - ^3\text{H}_6$ transition were studied in [7]. Pumping was performed by a laser diode into the 795-nm absorption band of Tm^{3+} with the absorption coefficient of about 7.5 cm^{-1} . It was found that cross relaxation processes can be efficiently used to produce the population inversion at the $^3\text{F}_4$ level of the Tm^{3+} ions in YAlO_3 crystals. However, pumping into the 795-nm absorption band is limited in power and does not allow one to obtain a high output power of the laser. A higher output power (up to 115 W) was achieved in [8], where a Tm^{3+} : YAG crystal ($C_{\text{Tm}} = 2\%$) of length 55 mm was used, which was longitudinally diode-pumped into the 804-nm absorption band with a significantly lower absorption coefficient. Of doubtless interest is the generation of high output powers in Tm^{3+} : YAlO_3 crystals longitudinally pumped by standard AlGaAs diodes in the region 803–805 nm.

In this paper, we studied the output characteristics of the Tm^{3+} : YAlO_3 laser ($C_{\text{Tm}} = 5.5\%$) emitting at the $^3\text{F}_4 - ^3\text{H}_6$ transition. The laser was pumped by an AlGaAs laser diode or laser diode array emitting in the region between 803 and 805 nm.

N.I. Borodin, P.V. Kryukov, A.V. Shestakov E.L.S. Co. Scientific and Production Center, ul. Vvedenskogo 3, 117342 Moscow, Russia; e-mail: nikbor1@rol.ru;

A.V. Popov, S.N. Ushakov Research Center of Laser Materials and Technologies, A.M. Prokhorov General Physics Institute, Russian Academy of Sciences, ul. Vavilova 38, 119991 Moscow, Russia; e-mail: Ushakov@lst.gpi.ru

Received 22 March 2005

Kvantovaya Elektronika 35 (6) 511–514 (2005)

Translated by M.N. Sapozhnikov

2. Absorption and luminescent characteristics of $\text{Tm}^{3+}:\text{YAlO}_3$ crystals

Tm^{3+} -doped yttrium aluminate single crystals were grown by the Czochralski method in the modified Kristall-3M growth setup with the automated control of growth and after-growth thermal processing parameters. Samples with $C_{\text{Tm}} = 1\%$ and 5.5% for spectral and lasing studies, respectively, were prepared from the grown crystals.

To determine the efficiency of cross relaxation processes, describing the population of the upper $^3\text{F}_4$ laser level, and the conditions for excitation of laser elements, we studied the polarisation absorption and luminescence spectra of $\text{Tm}^{3+}:\text{YAlO}_3$ crystals. The luminescence and absorption spectra were recorded with an SDL-1 spectrometer and an SF-20 spectrophotometer, respectively.

Figure 2 shows the polarisation absorption spectra of the $\text{Tm}^{3+}:\text{YAlO}_3$ crystal with $C_{\text{Tm}} = 5.5\%$ corresponding to the transition of the Tm^{3+} ions to the $^3\text{H}_4$ level for two orientations of the electric vector E of incident radiation with respect to the crystallographic axis c of the YAlO_3 crystal. One can see that for both polarisations, the intense 795-nm absorption band is observed. Along with this band, a number of absorption lines with the absorption coefficients $1\text{--}2\text{ cm}^{-1}$ are observed in the region $800\text{--}810\text{ nm}$, into which the pumping of active elements was assumed.

Because the efficiency of a Tm^{3+} -doped crystal laser emitting at $2\text{ }\mu\text{m}$ at $T = 300\text{ K}$ depends [9] on the efficiency of population of the $^3\text{F}_4$ metastable state due to cross relaxation (the $^3\text{H}_4 - ^3\text{F}_4$ and $^3\text{H}_6 - ^3\text{F}_4$ transitions), we studied the efficiency of this process in $\text{Tm}^{3+}:\text{YAlO}_3$ crystals with $C_{\text{Tm}} = 5.5\%$. By studying the luminescence decay from the $^3\text{H}_4$ level in the $\text{Tm}^{3+}:\text{YAlO}_3$ crystal with $C_{\text{Tm}} = 1\%$ at 300 K , we found that the decay is close to exponential. The dynamic range of the measured luminescence decay was four orders of magnitude [Fig. 3, curve (1)]. The lifetime of the excited $^3\text{H}_4$ level estimated in the time interval corresponding to this dynamic range was $500\text{ }\mu\text{s}$, which slightly differs from the value $630\text{ }\mu\text{s}$ measured at 77 K in [10]. As the concentration of Tm^{3+} ions in the YAlO_3 was increased up to 5.5% , luminescence from the $^3\text{H}_4$ level was strongly quenched [Fig. 3, curve (2)] due to cross relaxation ($^3\text{H}_4 - ^3\text{F}_4$, $^3\text{H}_6 - ^3\text{F}_4$). We estimated the cross relaxation efficiency $\beta_{\text{Tm} \rightarrow \text{Tm}}$ from the luminescence decay of Tm^{3+} ions. The efficiency was calculated from the expression [11]

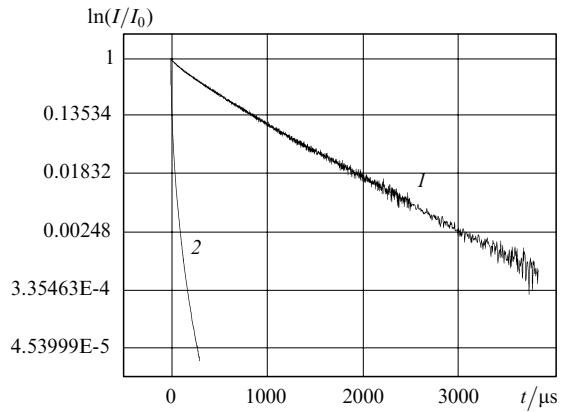


Figure 3. Luminescence decay curves for the excited $^3\text{H}_4$ level of Tm^{3+} ions in the YAlO_3 crystal (the excitation wavelength is 792 nm , the detection wavelength is 802 nm) for $C_{\text{Tm}} = 1\%$ (1) and 5.5% (2).

cence decay of Tm^{3+} ions. The efficiency was calculated from the expression [11]

$$\beta_{\text{Tm} \rightarrow \text{Tm}} = 1 - \int I_{\text{Tm}} dt / \int I'_{\text{Tm}} dt,$$

where I_{Tm} and I'_{Tm} are the intensities of luminescence of Tm^{3+} ions from the $^3\text{H}_4$ level in the presence and absence of cross relaxation, respectively. The result is presented in Table 1, where for comparison the value of $\beta_{\text{Tm} \rightarrow \text{Tm}}$ for YAG crystals is also given [12]

Table 1.

Crystal	$C_{\text{Tm}}(\%)$	$\beta_{\text{Tm} \rightarrow \text{Tm}}$
YAlO_3	5.5	98.5
	2.8	96
YAG	7.1	99

Our study showed that in $\text{Tm}^{3+}:\text{YAlO}_3$ crystals with $C_{\text{Tm}} = 5.5\%$ the cross relaxation efficiency responsible for the population of the upper $^3\text{F}_4$ laser level is high and can provide efficient lasing from this level in YAlO_3 crystals. Based on the spectral studies, we determined the dimensions of the $\text{Tm}^{3+}:\text{YAlO}_3$ crystals with $C_{\text{Tm}} = 5.5\%$ for investigations of lasing.

3. Lasing of longitudinally diode-pumped $\text{Tm}^{3+}:\text{YAlO}_3$ crystals

To investigate lasing, we fabricated from the $\text{Tm}^{3+}:\text{YAlO}_3$ crystal ($C_{\text{Tm}} = 5.5\%$) the active elements of dimensions $7, 7,$ and 5 mm along the $c, a,$ and b axes, respectively. The end faces of these elements perpendicular to the b axis were plane, and dielectric coatings of different types were deposited on them when different lasing schemes were used:

(i) A selective mirror with the reflectivity $R > 99.5\%$ at 1940 nm and the transmission coefficient $T > 85\%$ at 805 nm was deposited on one of the ends, while another end had an AR coating for 1940 nm (first type element);

(ii) a mirror highly reflecting at 1940 nm and transmitting 85% of pump radiation was deposited on the crystal end through which pumping was performed, while the output mirror with the transmission coefficient $T = 5.6\%$

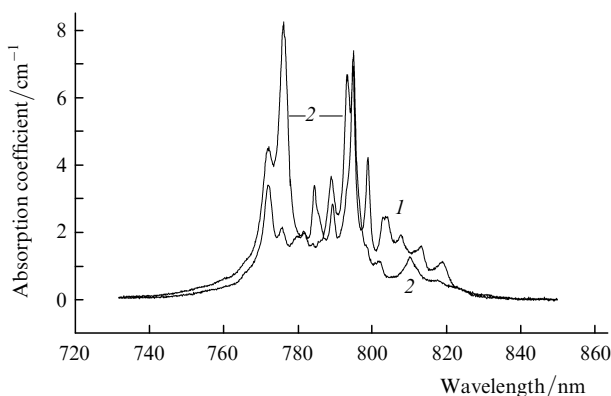


Figure 2. Polarisation absorption spectra of Tm^{3+} ions (the $^3\text{H}_6 - ^3\text{H}_4$ transition) in the YAlO_3 crystal ($C_{\text{Tm}} = 5.5\%$) at $T = 300\text{ K}$ for $c \parallel E$ (1) and $c \perp E$ (2).

at 1940 nm was deposited on another end (second type element).

We studied lasing of active elements pumped by a 2-W laser diode or a 30-W laser diode array (HLU30F400, LIMO GmbH). These elements were mounted in a copper housing whose temperature was varied between 15 and 25 °C with the help of a Peltier element. The first type active elements were used in lasers pumped by the laser diode array, and the second type active elements were used upon pumping by a laser diode.

3.1 Pumping by a laser diode

Radiation from a laser diode was focused into a 100×200 - μm spot on an active element by a lens with the focal distance $f = 3.3$ mm. The laser resonator was formed by mirrors deposited on the ends of the second type active element. Because radiation from the laser diode was polarised, the pump radiation and active element were mutually oriented taking into account the dependence presented in Fig. 2 [curve (2)]. The pump radiation wavelength was set to be 803 nm by varying the operating temperature of the diode.

Figure 4 shows the dependence of the output power of the laser on the pump power absorbed in the active element. The lasing threshold was achieved when the absorbed power was 0.7 W, the maximum output power was 540 mW for the absorbed pump power equal to 1.6 W. Therefore, the total lasing efficiency was 33 % and the slope efficiency was 60 %.

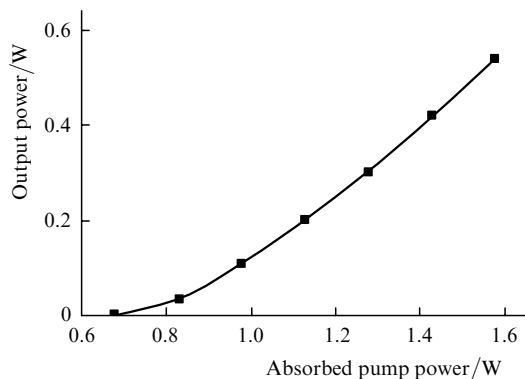


Figure 4. Dependence of the output power of the laser on the absorbed pump power upon pumping by a laser diode.

3.2 Pumping by a laser diode array

Radiation from a laser diode array with a fibre pigtail (the fibre diameter was 400 μm) was focused into a 0.65–0.67-mm spot on the first type active element by a $1.7\times$ four-lens condenser. The pump radiation in the region 802–805 nm at the fibre output was nonpolarised. The laser resonator was formed by a highly reflecting mirror deposited on the end face of the first type active element through which pumping was performed and by an external mirror with the transmission coefficient $T = 5.6$ %.

Figure 5 shows the output power of the laser with the output mirror with $T = 5.6$ % as a function of the absorbed pump power. The output power for the maximum pump power achieved 7.7 W. Analysis of the transverse distribution of the laser radiation field showed that only the TEM_{00} mode was excited in all cases. In this case, the total lasing

efficiency was 38.5 % and the slope efficiency was 45 %. For the pump power of 32 W achieved in our experiments, less than 20 W of pump radiation was absorbed in the active element during a round trip in the resonator, which suggests that the output characteristics can be improved by optimising the parameters of the active element and pump system. By using a double-pass pump scheme (Fig. 6), we obtained a higher output power for the same pump power due to the additional utilisation of a part of radiation transmitted through the active element. Thus, for the pump power of 32 W, the output power of the laser was 10.5 W.

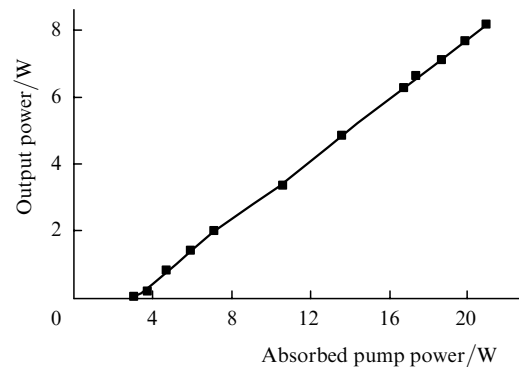


Figure 5. Dependence of the output power of the laser on the absorbed pump power upon pumping by a laser diode array.

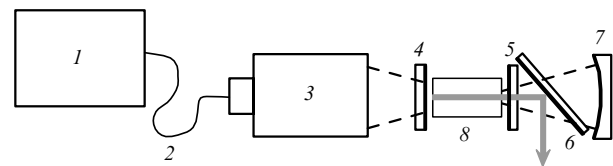


Figure 6. Optical scheme of the experiment with the use of double-pass pumping; (1) laser diode array; (2) optical fibre; (3) focusing system; (4–7) mirrors; (8) first type active element.

We measured the laser wavelengths at the ${}^3\text{F}_4 - {}^3\text{H}_6$ transition of Tm^{3+} ions in YAlO_3 crystals pumped by a laser diode or a laser diode array. The laser wavelength was measured with an MDR-23 monochromator with a spectral resolution of 3 nm. In both cases for $T = 5.6$ %, only one line at 1990 nm was generated. As the transmission of the output mirror is increased above 8 % and pumping is performed by a laser diode array, the laser wavelength changes to 1946 nm. In both cases, laser radiation is polarised so that the electric vector E is perpendicular to the c axis of the YAlO_3 crystal. Such a change in the laser wavelength is necessary for producing a large population inversion upon increasing radiative losses and a substantial change in the spectral dependence of the gain at the lasing transitions. We calculated using the method described in [13] the effective cross sections for the ${}^3\text{F}_4 - {}^3\text{H}_6$ lasing transition in Tm^{3+} ions for different polarisations of radiation and relative inverse populations P . The parameter P is defined as the ion density on the upper laser level divided by the active ion concentration. The results of calculations are presented in Fig. 7. One can see that for small values of the relative inverse population ($P < 0.17$), the 1990-nm line dominates, while at large value of

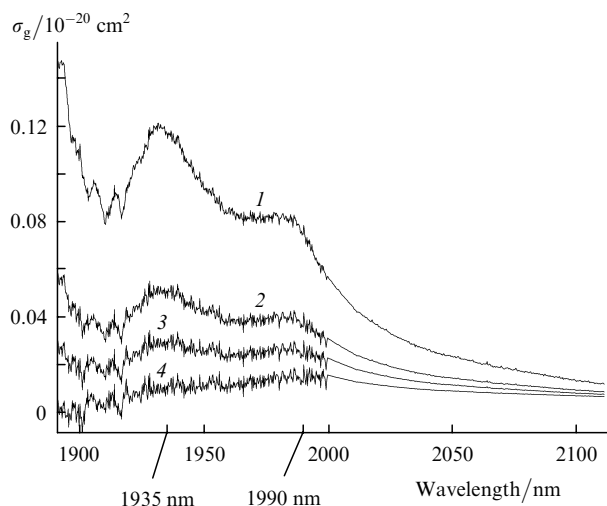


Figure 7. Spectra of the gain cross section σ_g for Tm^{3+} ions in the YAlO_3 crystal for $c \perp E$ and the relative inverse population $P = 0.50$ (1), 0.25 (2), 0.17 (3), and 0.10 (4).

$P \geq 0.17$, the 1935-nm line becomes dominant, in accordance with the experimental data.

4. Conclusions

We have demonstrated the efficient lasing of Tm^{3+} : YAlO_3 crystals longitudinally pumped into the 803–805-nm absorption bands by an AlGaAs laser diode or a diode array. A comparison of our results with the data obtained in [7] has shown that the lasing efficiency upon pumping by a laser diode into the 803-nm absorption band is comparable with that achieved in [7] upon pumping into the most intense 795-nm absorption band. The output power of 540 mW achieved when the absorbed pump power was 1.6 W corresponds to the result obtained in [7]. Upon pumping by the 32-W laser diode array, the maximum output power was 10.5 W for the pump radiation conversion efficiency equal to 32%–33%. It is shown that the optimisation of the parameters of the laser element and pump will improve the output characteristics of the Tm^{3+} : YAlO_3 crystal laser.

References

1. Ropoulos B. *Photon. Spectra*, June, 116 (1996).
2. Sudesh V., Piper J.A. *IEEE J. Quantum Electron.*, **36**, 879 (2000).
3. Stoneman R.C., Esterovitz L. *IEEE J. Sel. Top. Quantum Electron.*, **1**, 78 (1995).
4. Noginov M.A., Pokhorov A.M., Sarkisyan G.K., Smirnov V.A., Shcherbakov I.A. *Kvantovaya Elektron.*, **18**, 1042 (1991) [*Sov. J. Quantum Electron.*, **21**, 945 (1991)].
5. Payne S.A., Chase L.L., Smith L.K., Kway W.L., Krupke W.F. *IEEE J. Quantum Electron.*, **28**, 2619 (1992).
6. Kaminsky A.A. *Laser Crystals: Their Physics and Properties* (Berlin: Springer, 1981; Moscow: Nauka, 1975).
7. Elder I.F., Payne J. *Appl. Opt.*, **36**, 8606 (1997).
8. Honea E.C., Beach R.J., Sutton S.B., Speth J.A., Mitchell S.C., Skidmore J.A., Emanuel M.A., Payne S.A. *IEEE J. Quantum Electron.*, **33**, 1592 (1997).
9. Antipenko B.M., Buchenkov A.S., Kiseleva T.I., Krutova L.I., Nikitichev A.A., Pis'mennyi V.A. *Pis'ma Zh. Tekh. Fiz.*, **15**, 80 (1989).
10. Ivanov A.O., Mochalov I.V., Tkachuk A.M., Fedorov V.A., Feofilov P.P. *Kvantovaya Elektron.*, **2**, 188 (1975) [*Sov. J. Quantum Electron.*, **5**, 117 (1975)].
11. Voron'ko Yu.K., Gessden S.B., Es'kov N.A., Ryabochkina P.A., Sobol' A.A., Ushakov S.N., Tsybal L.I. *Kvantovaya Elektron.*, **20**, 363 (1993) [*Quantum Electron.*, **23**, 309 (1993)].
12. Becker T., Clausen R., Huber G., Duczynski E.W., Mitzscherlich P. *OSA Proc. Tunable Solid State Lasers*, **5**, 150 (1989).
13. Ryba-Romanowski W., Golab S., Sokolska I., Dominiak-Dzik G., Zawadzka J., Berkowski M., Fink-Finowicki J., Baba M. *Appl. Phys. B*, **68**, 199 (1999).